Electronic Supplementary Material (ESI) for Environmental Science: Nano.

Supporting information

Insight into the Pressure-induced Displacement Mechanism for Selecting Efficient Nanofluids in Various Capillaries

Xiao Wang [1], Zhiliang Zhang [1], Jun Zhang [2] and Jianying He [1,*]

[1] NTNU Nanomechanical Lab, Department of Structural Engineering, Faculty of Engineering, Norwegian University of Science and Technology (NTNU), 7491 Trondheim, Norway

[2] School of Materials Science and Engineering, China University of Petroleum, Qingdao, Shandong, 266580 China

* Correspondence: jianying.he@ntnu.no ; Tel.: +47-93804711

S1. Adsorption Behavior of Decane

The orientation of decane is important to understand the displacement process. Here, the orientation of decane molecules at capillary wall and water-oil interface are analyzed separately. For decane adsorption on capillary wall, the equilibrium configuration is captured from the trajectory of molecular dynamics simulations. As shown in Figure S1, the decane molecules exhibit an obvious layer by layer adsorption on capillary. This phenomenon is consistent with our previous works and other simulation studies [1, 2].

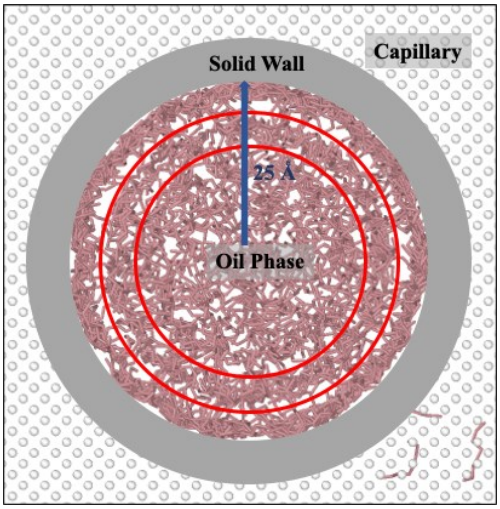

Figure S1 The adsorption configuration of oil phase in capillary. The gray color represents the solid wall of the capillary. The red lines depict the adsorption layers of decane molecules in the capillary.

Meanwhile, the orientation of decane with respect to the dynamical oil/water interface is analyzed qualitatively by the equilibrium configurations. The hydrophobic capillary is taken as an example. As shown in Figure S2(a) and (b), the oil/water interface in hydrophobic capillary can be divided into two parts, i.e., the interfaces near (cyan, Part I) and away from (yellow, Part II) the capillary. For Part I, during the flooding process, decane always adsorbs parallel to the solid surface due to its strong interaction with hydrophobic wall (Figure S2(b)). However, for part II, different orientations are observed (Figure S2(c)), i.e., normal to interface (blue), parallel to interface (yellow), and tilted to the interface (green). Moreover, along with the simulation time, decane molecules involve large diffusions, and their orientations change randomly.

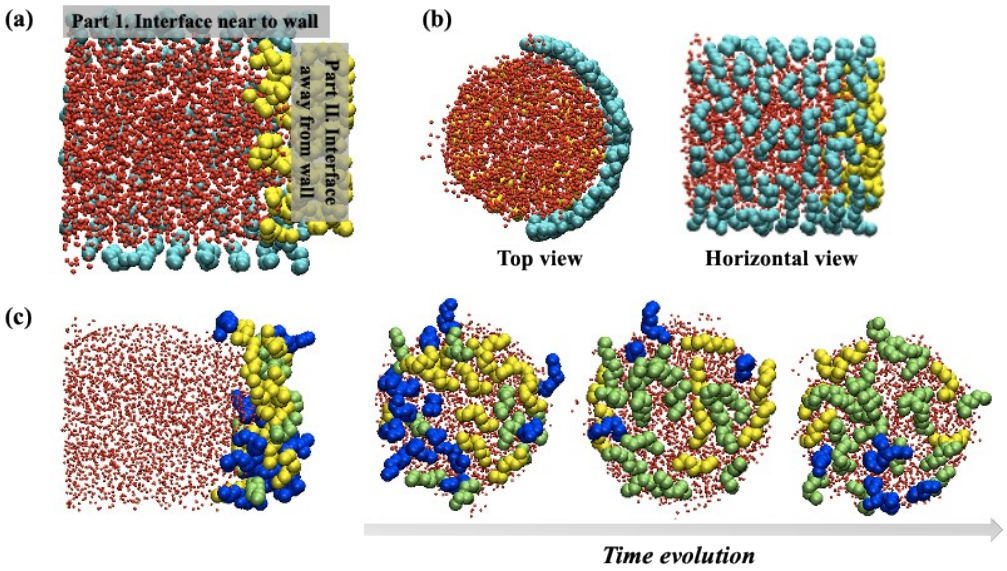

Figure S2 Configurations of water-oil interface in the nanochannel. (a) water-oil interface; (b) top view and horizontal view; (c) Part II from horizontal view and top views; The colors in (a) and (b): water (red); oil in part I (cyan); oil in part II (yellow); The colors in (c); water (red); oil normal to interface (blue), oil parallel to interface (yellow) and oil tilted to interface (green).

S2. Verification of Model

The fluids properties in the system are verified by viscosity of water and interfacial tension of decane/water. This process is also described in our previous simulations.

The viscosity of water can be derived by Einstein relation [2, 3].

$$\eta = \frac{k_B T}{3\pi r_w} \frac{1}{D} \tag{S1}$$

where k_B is the Boltzmann constant, T is simulation temperature, r_w is the molecular diameter, and D is diffusion coefficient of fluid. According to previous simulation, self-diffusion coefficient for water is $2.67\times10^{-9}m^2s^{-1}$, which matches well with experimental data ($2.09\text{-}2.66\times10^{-9}m^2s^{-1}$) and other simulation results [4]. The calculated viscosity of water is 0.9622 MPa·s under 298.15 K using Eq.S1, in good agreement with experimental value of 1.0 MPa·s. The other important property is water-oil interfacial tension. The interfacial tension of water-oil is derived by subtracting mean tangential stress tensors (i.e., P_{xx} and P_{yy}) from the normal one (i.e., P_{zz}) [5].

$$\sigma_{wo} = \frac{1}{2} L_z \left\langle P_{zz} - \frac{1}{2}(P_{xx} + P_{yy}) \right\rangle \tag{S2}$$

where L_z is the length of simulation box in z axis. The calculated interfacial tension for decane/water interface is 50.54±1.28 mN/m, in good agreement with the experimental value of 51.98 mN/m [6].

S3. Three-phase Contact angle

To calculate three-phase contact angle to assess the wettability of capillary, the water and oil were initially placed into the capillary, and the piston was fixed. Here, the characteristic energy ε_{sw} was tuned from 0.1 to 0.4 kcal/mol, forming hydrophobic to hydrophilic capillary, and other parameters were kept the same as those in Section 2. The detailed configuration is shown in Figure S3. The 4.0 ns simulation time was adopted to equilibrium the system, and the last 2.0 ns was analyzed to calculate three-phase contact angle.

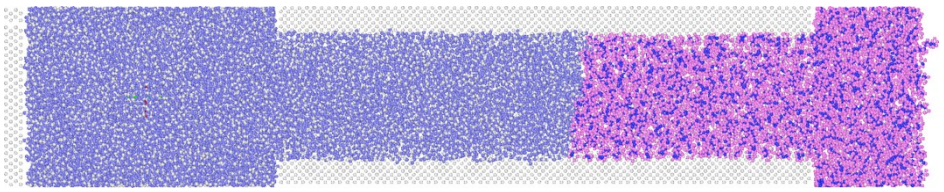

Figure S3 Simulation model to calculate three-phase contact angle in different capillary. The colors in Figure: piston and capillary (white); water (blue); oil (purple and blue).

According to our previous study, [7] contact angle will have large fluctuation and reach a dynamic equilibrium value during displacement. To determine the contact angle, liquid in capillary is firstly divided into cylindrical shells, and then is subdivided by certain thickness 1.5 Å. The number of shells should be constrained to ensure that each shell contains enough water molecules to give a uniform density. The density of water in each shell as a function of the distance l into the pore is analyzed. The advancing end of each shell is located at where the

density is below a cutoff value of half the water density. The contact angle is then obtained from the tangent to a circular fit to the profile. [7] Here, the three-phase contact angle in capillary with ε_{sw} = 0.1 kcal/mol is shown in Figure S4. From Figure S4, it can be seen that contact angle for fluids in the capillary is almost stable, and the relative equilibrium value can be obtained. The same method can be applied to other capillary and the results are in the Figure 4(b) in the main text.

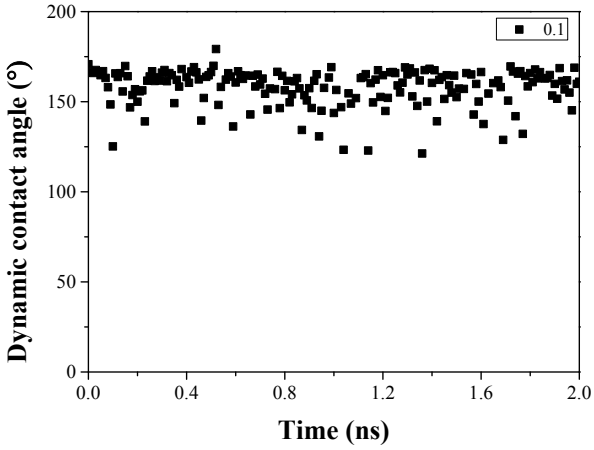

Figure S4 Dynamic three-phase contact angle for fluids in capillary with ε_{sw} = 0.1 kcal/mol.

S4. Relationship between position of piston and threshold capillary pressure

Figure S5 is a schematic diagram about two-phase displacement process in the nanochannel. During the fluid flow process, there will be viscous force, capillary force and external force in this system. During the fluid flow process , the force balance can be described as Eq.S3[8].

$$P_{applied} = \frac{2\gamma_{AB}\cos\theta}{R} - \frac{8\eta_A}{R^2} l_A \frac{dl_A}{dt} - \frac{8\eta_B}{R^2} l_B \left(- \frac{dl_B}{dt} \right) \tag{S3}$$

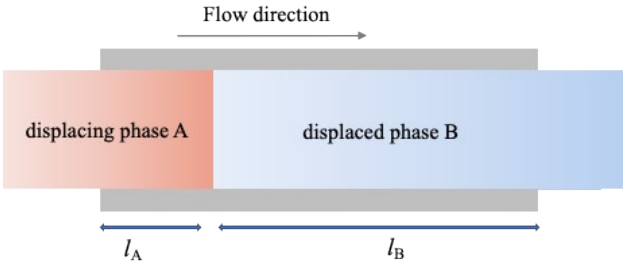

Figure S5 The schematic for two-phase displacement process in nanochannel

where $P_{applied}$ is applied force, γ_{AB} is interfacial tension between A and B, θ is three-phase contact angle, R is capillary radius, η_A and η_B are viscosity of phase A and B, resperctivley. l_A and l_B are length of phase A and B in capillary, and t is simulation time.

Considering no velocity for displacing phase A and B at the equilibrium state, then the equation can be simplified to

$$P_{threshold} = \frac{2\gamma_{AB}\cos\theta}{R} \tag{S4}$$

From Eq.S4, it can be seen that the threshold capillary pressure only relates to the interfacial tension γ_{AB} , contact angle θ, and capillary radius R, which it is not affected by the position of the piston.

S5. Influence of pumping pressure on forced displacement process in capillary

For the influence of pumping pressure on the forced displacement process, the configurations of forced water-oil displacement in varied capillary under different pumping pressure are shown in Figure S6.

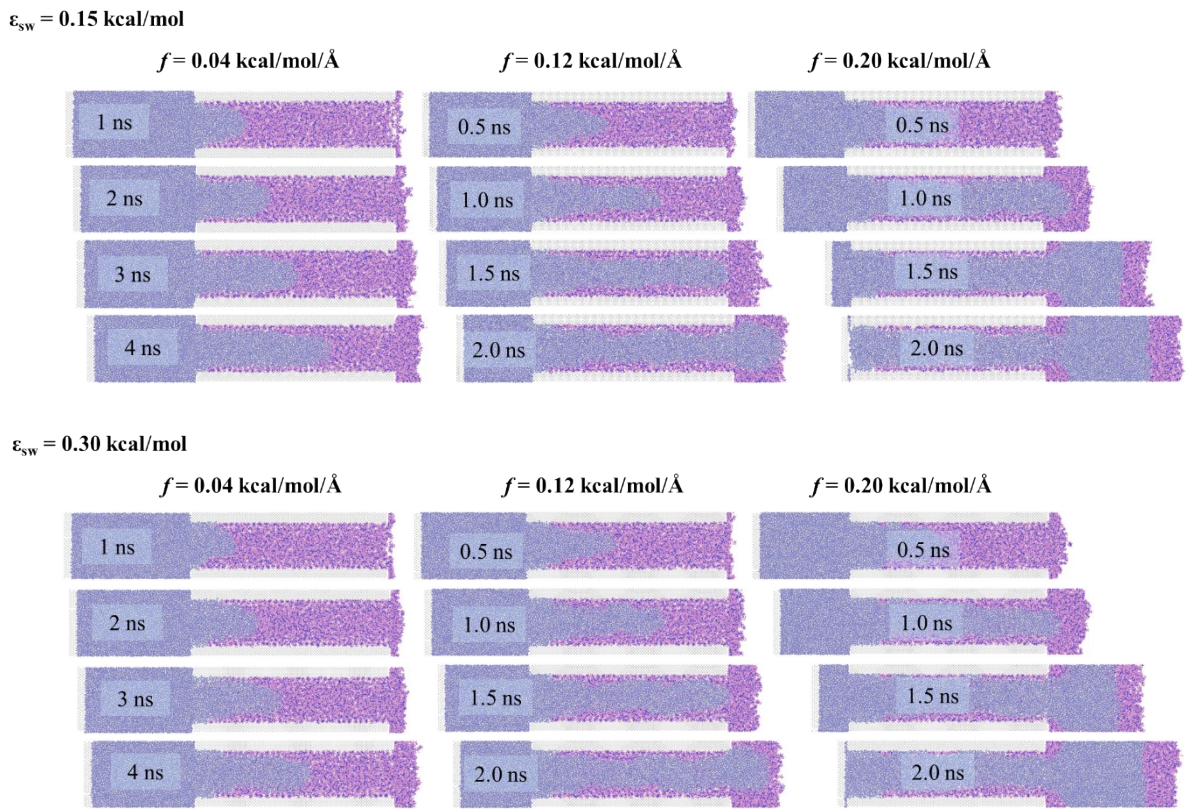

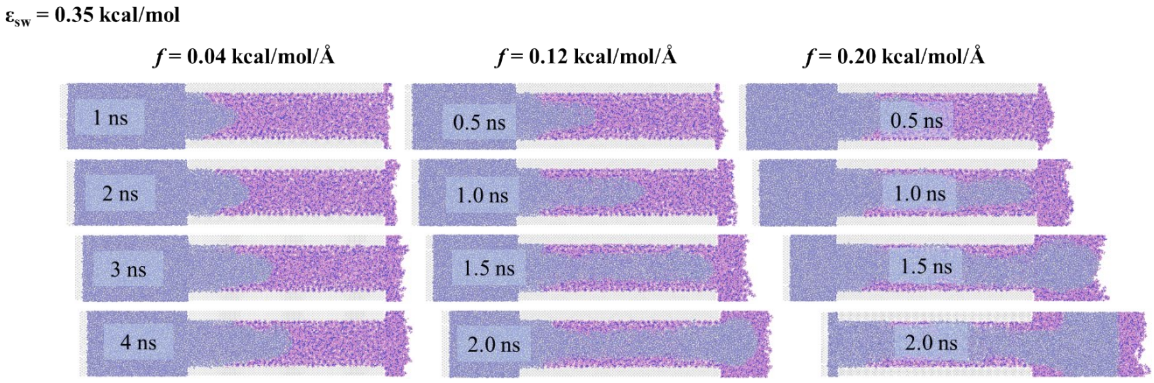

Figure S6 Flow snapshots for forced water-oil displacement in different kinds of capillary under different pumping pressure. The colors are the same as in Figure S3.

S6. Simulation details of forced displacement by nanofluids

To study the influence of nanoparticles on the forced displacement process, 16 spherical NPs with a diameter of 7.0 Å were well distributed in water phase. The main characteristic energies for NPs are interactions with water ε_{nw} and NP-NP ε_{nn}, The characteristic energy for NP-NP ε_{nn} was set relatively small as 0.01 kcal/mol for a weak interaction between NPs. And ε_{ns} was chosen 0.7 kcal/mol designating the strong interaction between solid capillary and NPs. By tuning characteristic energy ε_{nw} between NPs and water, hydrophobic, Janus, and hydrophilic NPs were obtained, listed in Table S1. Then other parameters were kept the same as in the main text [2, 9].

Table S1 Force fields parameters for NPs with water ε_{nw}, oil ε_{no}, and capillary ε_{ns}.

Characteristic energy, kcal/mol	Water	Oil	Capillary
Hydrophilic NPs	0.6	0.05	0.7
Janus NPs (hydrophobic)	0.01	0.2	
Janus NPs (hydrophilic)	0.4	0.01	
Hydrophobic NPs	0.05	0.6	

S7. Displacement mechanism of nanoparticles in capillary

Via analyses of displacement length, motion behavior and capillary pressure etc. in our previous simulations [2, 9], displacement mechanisms of different NPs during displacing process are summarized in Figure S7. In Figure S7, the first line is the type of NPs. The second line

shows the motion behavior for NPs in capillary, i.e., dispersed in water, adsorbed onto capillary, aggregated bigger micelles, or self-assembled at fluids interface. The last line gives the dominating displacement mechanism for NPs displaced in capillary.

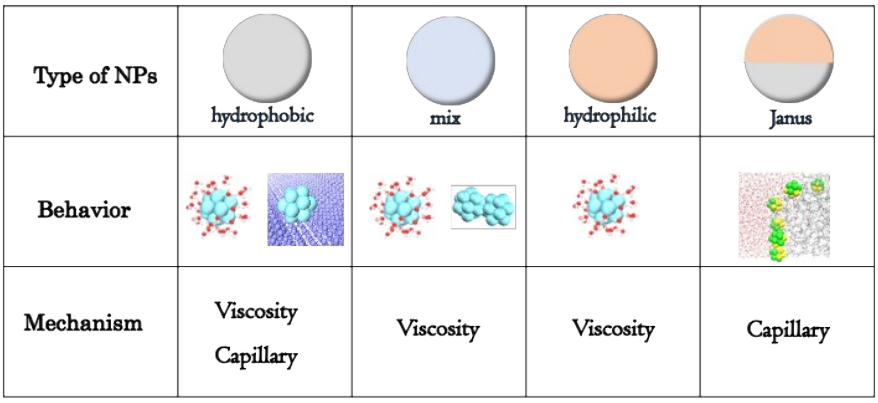

Figure S7 Summarized of the motion behavior and displacement mechanism of different NPs in capillary.

References

1. H. Yan and S. Yuan, Molecular Dynamics Simulation of the Oil Detachment Process within Silica Nanopores, *J. Phys. Chem. C.*, 2016, **120**, 2667-2674.

2. X. Wang, Z. Zhang, O. Torsaeter and J. He, Atomistic insights into the nanofluid transport through an ultra-confined capillary, *Phys. Chem. Chem. Phys.*, 2018, **20**, 4831-4839.

3. J. A. Thomas and A. J. H. McGaughey, Reassessing Fast Water Transport Through Carbon Nanotubes, *Nano Lett*, 2008, **8**, 2788-2793.

4. Y. Yan, X. Wang, Y. Zhang, P. Wang, X. Cao and J. Zhang, Molecular dynamics simulation of corrosive species diffusion in imidazoline inhibitor films with different alkyl chain length, *Corros. Sci.*, 2013, **73**, 123-129.

5. Y. Zhang, S. E. Feller, B. R. Brooks and R. W. Pastor, Computer simulation of liquid/liquid interfaces. I. Theory and application to octane/water, *J. Chem. Phys.*, 1995, **103**, 10252-10266.

6. F. Leroy, Revisiting the droplet simulation approach to derive force-field parameters for water on molybdenum disulfide from wetting angle measurements, *J. Chem. Phys.*, 2016, **145**, 164705-164716.

7. X. Wang, S. Xiao, Z. Zhang and J. He, Effect of Nanoparticles on Spontaneous Imbibition of Water into Ultraconfined Reservoir Capillary by Molecular Dynamics Simulation, *Energies*, 2017, **10**, 506.

8. C. Chen, K. Lu, X. Li, J. Dong, J. Lu and L. Zhuang, A many-body dissipative particle dynamics study of fluid–fluid spontaneous capillary displacement, *RSC Advances*, 2014, **4**, 6545-6555.

9. X. Wang, S. Xiao, Z. Zhang and J. He, Transportation of Janus nanoparticles in confined nanochannels: a molecular dynamics simulation, *Environ. Sci.: Nano*, 2019, **6**, 2810-2819.